LIQUID METAL HEAT SINK FOR LAPTOP COMPUTERS

A Thesis

presented to

the Faculty of the Graduate School

at the University of Missouri-Columbia

In Partial Fulfillment

of the Requirements for the Degree

Master of Science

---

by

CHENGYI GU

Dr. Matthew Maschmann, Thesis Supervisor

MAY 2017

The undersigned, appointed by the dean of the Graduate School, have examined the thesis entitled

LIQUID METAL HEAT SINK FOR LAPTOP COMPUTERS

Presented by Chengyi Gu,

a candidate for the degree of Master of Science,

and hereby certify that, in their opinion, it is worthy of acceptance.

_____

Assistant Professor Matthew Maschmann

_____

Professor Hongbin Ma

_____

Professor Rainer Glaser

ACKNOWLEDGEMENT

I would first like to appreciate my advisor and committee chair, Dr Matthew Maschmann. The door to Dr Maschmann's office was always open whenever I ran into a trouble spot or met problem about my research or writing. He consistently allowed this thesis to be my own work, but steered me in the right direction.

I would also like to thank Dr Hongbin Ma for this awesome research topic. He became a great source for general advice on my graduate studies. Without his guidance and help, this thesis can not be successfully conducted.

I would also sincerely thank Dr Rainer Glaser for serving on my committee and for his time and efforts to help me in innumerable ways.

I would also like to use this chance to thank Ethan Bruzzese, Minwoo Lee and my colleages for their great helping and caring they provided when I met difficulty.

Finally, I extend the warmest appreciate to my parents who have always encouraged me during my studying life and Hui Chen who gives me love and support at the end of my student life. Hope you can get your PhD degree as soon as possible.

Table of Contents

LIST OF FIGURES

List of Tables

ABSTRACT

With the rapid miniaturization of the electronic systems, heat generation in the components becomes a major concern for thermal management. The high density of heat generation can be a bottleneck to attain higher performance and reliability of computers. Because conventional cooling methods such as finned heat sink are often incapable of providing adequate cooling for sophisticated electronic systems, new systems like heat pipes or liquid cooling systems are being studied. This work focused on the novel design of a liquid metal and heat sink cooling loop targeted for laptop computer thermal management. The liquid metal was driven by an electromechanical pump, offering no moving parts and quiet operation. To better understand the design process, theoretical analysis for fluid flow and heat transfer performance of liquid metal and heat sink are conducted. Furthermore, in order to demonstrate the feasibility of this new concept, a series of experiments on the fabricated module under different heater powers and pump power are performed. A thermal resistance value of 0.53 °C/W was experimentally determined, making the performance similar to competing technologies. Performance was impeded by a low pump efficiency, a known impediment with electromagnetic pumps.

Chapter 1 Introduction

1.1 Thermal Problem for CPU Chip

The trend towards increased transistor density is a tremendous concern for thermal management, as power density of components has continued to increase. Furthermore, the form factor of digital devices has continued to decrease with the advent of tablet computers and very thin laptops. Maintaining a reduced form factor while adequately removing modest heat fluxes from multiple components is an issue of significant importance. For these systems, conventional metallic heat sinks alone are insufficient to meet the thermal and design constraints, so more advanced cooling solutions have been utilized.

1.2 Heat Pipes

Conventional copper and aluminum finned heat sink have drawbacks such as poor cooling performance, acoustic noise increase and weight rise. To address the enhanced thermal performance requirements demanded by conventional electronic devices, a remote heat sink integrated with a heat pipe was proposed. The conventional heat pipe (CHP) as seen in Figure 1.1 is a heat transfer device that effectively utilizes evaporation and condensation to transfer heat for a long distance. Due to its low cost and much higher effective thermal conductivity which is about 10,000W/m-K. Copper, considered the top performing metal for thermal management devices, has a thermal conductivity of 400W/m-K. CHPs are already commonly used for PC and laptop cooling.

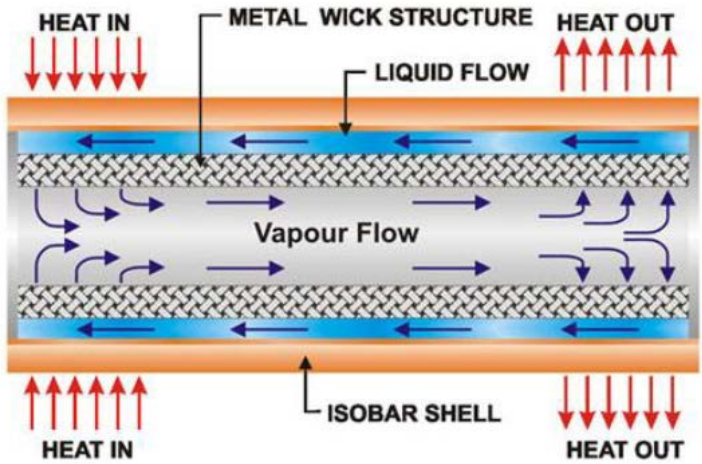

Figure 1.1. Schematic of conventional heat pipe

Kim, Won and Back developed coolers using heat pipes for the Pentium-IV generation of CPUs to reduce fan revolution speed and reduce acoustic noise in 2003[1]. Thermal stability of the cooling device was tested using the experimental set-up shown in Figure 1.2, with additional device configurations shown in Figure 1.3. The results from this testing demonstrated that the heat pipe cooling device had better cooling performance than a conventional heat sink at a low speed below 2950 rpm. This performance advantage enabled it to be applied as a cooling system offering low acoustic and high performance where an aluminum finned heat sink could not meet the required specifications.

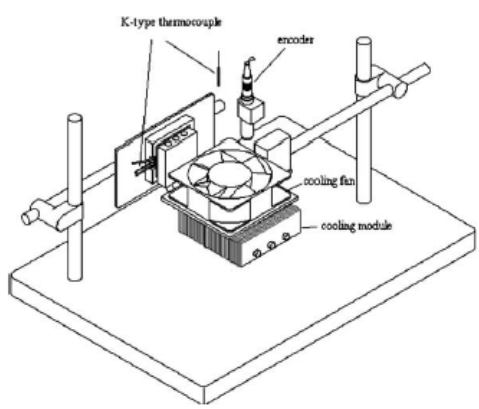

Figure 1.2. Schematic diagram of experimental set-up [1]

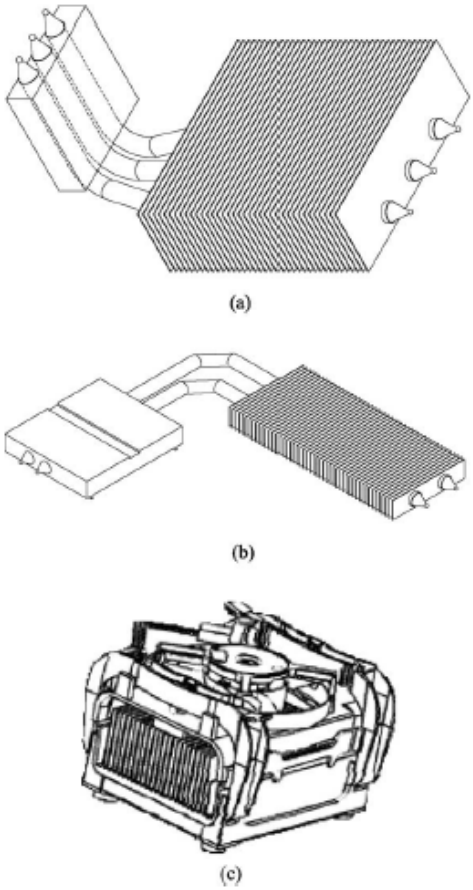

Figure 1.3. Three types of cooling devices: (a) Remote Heat Exchanger I (top heating mode), (b) RHE II (bottom heating mode) and (c) heat sink (Intel's boxed cooler) [1]

However, the considerable increase of heat flux generated from more advanced electronic components causes new demand which cannot be met by CHPs. Thus, a more highly efficient heat transfer device based on a similar operation principle was introduced to further enhance performance. A loop heat pipe (LHP) is shown in Figure 1.4. The LHP has the advantages of much higher heat capacity at suitable dimensions, lower thermal resistance and flexibility in packaging. The merits of LHPs over CHPs are more obvious when dealing with high heat flux over long distances, especially if heat transfer is required

in an opposite tilt condition [2]. For applications requiring a more compact space, miniature loop heat pipes (MLHPs) are utilized.

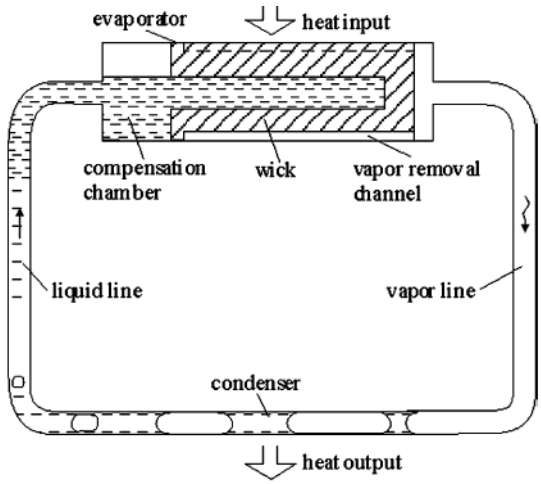

Figure 1.4. Principal Scheme of an LHP [2]

In 2002, Pastukhov and Maidanik developed MLHPs with a cooling capability of 25-30W and a heat transfer distance up to 250 mm. The device was used for cooling CPU chip and other electronic components [3]. Three prototypes of M and L shape MLHPs incorporated into remote heat exchanger (RHE) were investigated under various circumstances. The results are obtained under air cooling produced a total thermal resistance of 0.3-1.2 °C/W, with values strongly dependent on the cooling conditions and the radiator efficiency. These results above make it possible to consider MLHP as promising devices for electronic components cooling.

Oscillating heat pipes (OHPs) have also become as another interesting alternative to CHP because they offer high heat transport capability, gravity independence, and excellent form factor and manufacturing. An OHP is a self-contained device that features internal channels that are partially filled with a liquid coolant. The remaining volume represents the coolant vapor phase. Upon heating, additional vapor is formed in the heated

section, while condensation occurs in the cooled section on the opposite side of the device. The net result is an oscillating motion of the coolant that further enhanced heat transfer performance. Akachi was the first to develop this heat transfer device which can be confirmed from his 1990 [4] and 1993 [5] patents. Over the last several decades, extensive researches on OHP have been implemented leading to a large amount of articles published about OHP and its application. By design, OHPs were divided by two categories: open loop OHP (OLOHP) and close loop OHP (CLOHP) shown in Figure 1.5. According to open literature, it is hard to reach an accurate conclusion as to which of these two types of OHP is superior. The experience of the researchers themselves illustrates that the main difference between the function of a CLOHP and an OLOHP is related with the minimum value of the power required to initiate start-up (or oscillating behavior). Prior to the start-up, thermal performance of the device is poor. Because of this, the thermal load required for star-up latter is a significant concern that may be equal to or greater than thermal performance during oscillation.

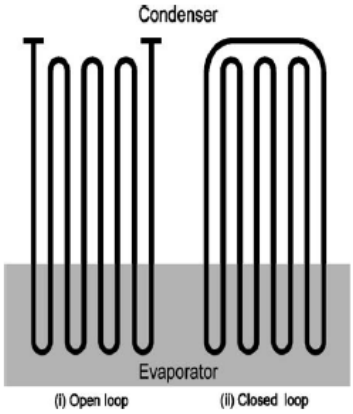

Figure 1.5. Two Configurations of OHP: (1) Open loop (2) Close loop [6]

The simplicity of the design, incorporation with sufficient heat transport characteristics and the possibility of different design specifications, makes OHPs an

emergent technology for actual application [7]. Maydanik, Dmitrin and Pastukhov (2009) developed and studied a compact cooler for electronics combined with a closed loop oscillating heat pipe because of the lower heat loads than open loop [7]. The scheme of 3D OHP and appearance view of a cooler is shown in Figure 1.6 and 1.7. The operation of

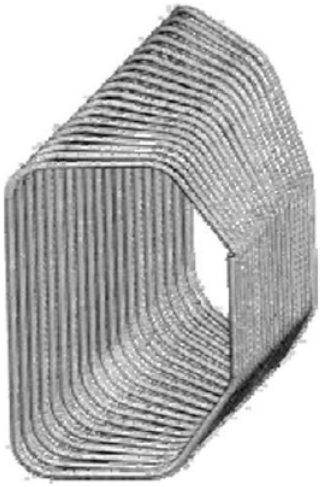

Figure 1.6. Scheme of 3D OHP [7]

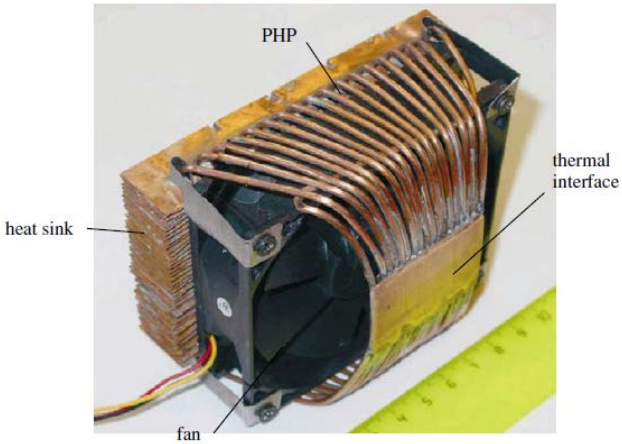

Figure 1.7. External view of a cooler with CLOHP [7]

the cooler was conducted with water, methanol and R141b as working fluids at a uniform and concentrated supply of a heat load in the range of 5 to 250W. The smallest "heat source-ambient air" thermal resistance value obtained from the experiment results equals to

0.32℃/W when water and methanol were working fluids at a uniform heat power of 250W. With a heat load concentrated on a section of the thermal interface restricted in an area of 1cm^2, the minimum value of thermal resistance attained is 0.62℃/W at a heat load of 125W when methanol was used as the working fluid. Attractive applications based on OHP have been suggested for cooling CPU chip as well. In 2005, Rittidech, Boonyaem and Tipnet designed and established an experimental prototype to test the cooling performance of a closed-end oscillating heat pipe (CEOHP) [8]. The prototype and test apparatus are shown in Figure 1.8 and 1.9. The comparison tests were performed with conventional heat sink. The experimental data demonstrated that the CEOHP had better cooling performance than conventional aluminum finned heat sink. What's more, the increase of the fan speed can enhance the cooling capacity and improve the thermal performance better.

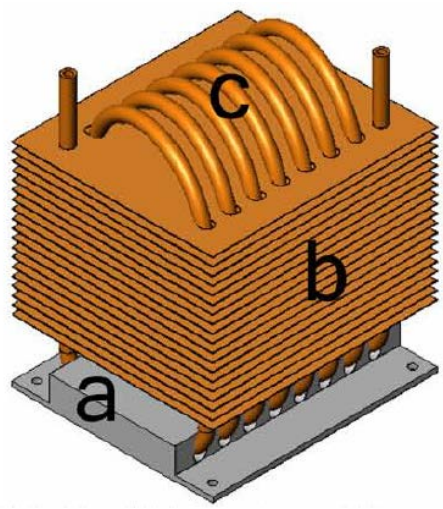

Figure 1.8. Prototype: (a) aluminum base plate (b) copper fins (c) CEOHP [8]

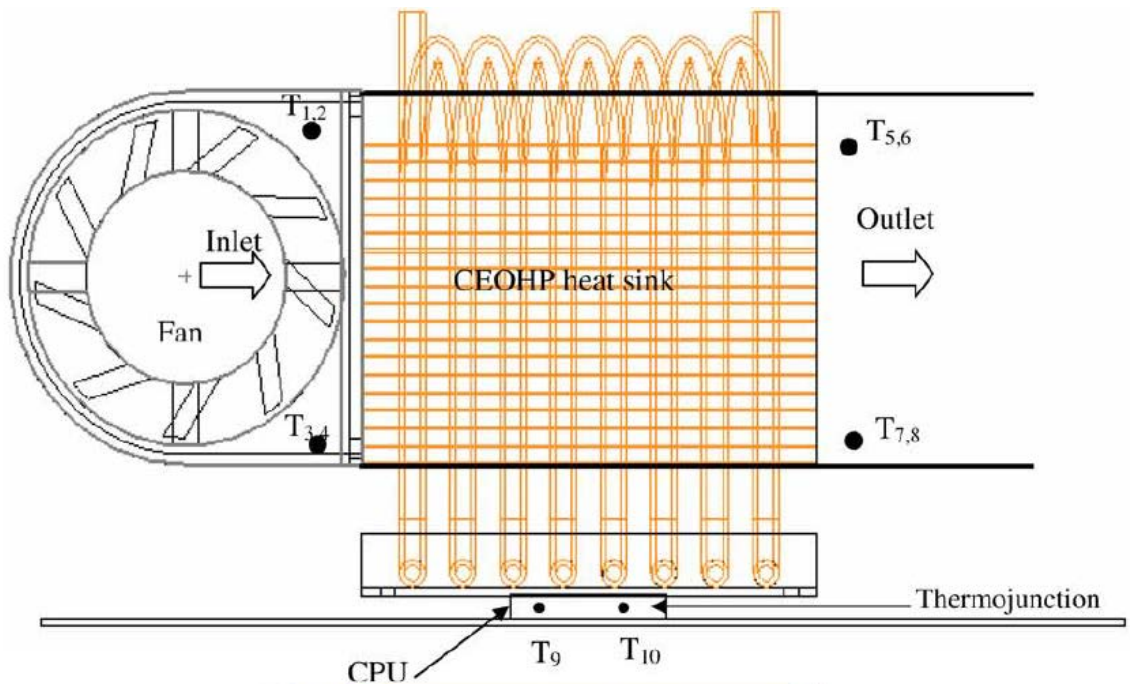

Figure 1.9. Schematic of test apparatus [8]

1.3 Water Cooling System

The high heat flux generated from high-performance CPU chips have already extended the cooling requirements beyond those achievable for heat pipes, forced air cooling, etc. Liquid cooling systems are another approach of heat removal from electronic components and industrial equipment. Here, internal liquid flow provides forced convection that can efficiently cool thermal systems. A radiator then rejects the heat remotely before the water is re-circulated to the heated components. Among all of the liquid cooling systems, water is the most common working fluids. The advantages of using water cooling over air cooling include high specific heat capacity and thermal conductivity. These features allow water to transport heat over larger distance at reduced flow rate and temperature differences. For CPU chip cooling, the critical merits of water cooling is that it is capable of transmitting heat away from the source to another cooling surface which

allows larger and more desired radiators instead of smaller, relatively inefficient fins mounted directly on the heat source. Zeng and Cheng investigated the performance of composite water cooling system on CPU chip in 2005 [9]. This water cooling system is driven by piezoelectric pump with two parallel-connected chambers and the mechanism and structure of piezoelectric pump with two parallel-connected chambers are depicted. It is found that the performance of water cooling system is much higher than that of air-cooled heat sinks according to the comparison test results. The thermal equilibrium temperature is 6℃ lower and it enables to shorten 35 mins to reach steady state.

1.4 Limitations for heat pipe and water cooling system

Although the advanced cooling systems facilitate significantly greater heat transfer than traditional finned heat sinks, there are also numerous other considerations to investigate. For example, the application of heat pipe is mainly limited to transferring comparatively small heat load over relatively short distance when the evaporator and condenser are at same horizontal level. This limitation on the part of heat pipes is mainly connected to the major pressure loss associated with the liquid flow through the capillary structure, present along the entire length of the heat pipe. An additional pressure loss occurs by viscous interaction between the vapor and liquid phases, also called entrainment losses. For the applications involving large heat load transfer over long distance, the thermal performance of the heat pipes is significantly decreased by these losses. Because of the same reason, conventional heat pipes are very sensitive to the change in orientation in gravitational field. For an unfavorable slope in the evaporator-above-condenser configuration, the pressure losses due to the mass forces in gravity field adds to the total

pressure losses and further lower the efficiency of the heat transfer process. In order to solve these limitations, new types of heat pipes have already been proposed such as, loop heat pipe, oscillating heat pipes, etc. Though these new forms of heat pipes are able to transfer significant heat flows and can increase heat transport length, they still remain very sensitive to spatial orientation relative to gravity.

Water cooling system is more efficient than heat pipes to some extent. However, there are also some demerits we need to take into consideration. Water is non-toxic but it can accelerate the corrosion of a metal part and can damage circuitry if it is accidentally released. Dissolved minerals in water supply are aggregated by evaporation to leave deposits which could damage the system. Furthermore, a large-size heat exchanger is necessary for effective heat transfer from the heat source because of the low thermal conductivity of water compared with liquid metal. The common driving pumps usually have poor reliability and mechanical problems. In the case of using electro osmotic pumps, high electrode potential may dissociate the water molecules.

1.5 Liquid metal cooling

Due to the limitations illustrated above, miniaturization on heat exchanger and improvement of thermal properties of coolants calls for the advent of alternative candidates for liquid cooling system. In 2002, Liu and his research group used liquid metal alloy for CPU chip cooling [10, 11]. Later work by Miner and Ghoshal supports this proposal further [12]. Liquid metal can offer a unique solution for cooling high density heat sources and transferring heat in a limited space. The two primary advantages lie in their excellent thermo-physical properties for absorbing and transporting heat, and in the ability to pump

these fluids effectively with a silent, vibration free, low energy cost, non-moving and compact electromagnetic pump due to its high thermal and electrical conductivity [12].

1.5.1 Thermo-physical properties of liquid metal

As a practical coolant for computer chips, the liquid metal must have a low melting point, a low viscosity, a high thermal and electric conductivity and a high heat capacity. Meanwhile, it must be non-toxic and non-corrosive. The liquid metal should also maintain a liquid state at all times during operation. Compared with various liquid metals, it is easily to find that the liquid gallium or its alloys should be considered as a best candidate for coolant which has already been well known in the area of cooling nuclear reactors [13]. Table 1.1 lists the thermo-physical properties of typical liquid metals [14].

Table 1.1. Thermo-physical properties of typical liquid metals with low melting point [14]

Liquid metals	Melting point/°C	Evaporation point/°C	Evaporation pressure/mmHg	Specific heat /kJ·(kg·K)$^{-1}$	Density/kg·m^{-3}	Thermal conductivity /W·(m·°C)$^{-1}$	Surface tension /N·m^{-1}
Mercury	–38.87	356.65	1.68×10^{-3} a)	0.139 a)	13 546 a)	8.34 a)	0.455 a)
Cesium	28.65	2 023.84	10^{-6} d)	0.236 d)	1 796 d)	17.4 d)	0.248 d)
Gallium	29.8	2 204.8	10^{-12}	0.37 n)	5 907 n)	29.4 n)	0.707 n)
Rubidium	38.85	685.73	6×10^{-6}	0.363 m)	1 470 m)	29.3 m)	0.081
Potassium	63.2	756.5	6×10^{-7}	0.78 m)	664 m)	54.0 m)	0.103 d)
Sodium	97.83	881.4	10^{-10}	1.38 d)	926.9 d)	86.9 d)	0.194 d)
Indium	156.8	2 023.8	$< 10^{-10}$	0.27 m)	7 030 c)	36.4 c)	0.55 m)
Lithium	186	1 342.3	10^{-10}	4.389 b)	515 b)	41.3 b)	0.405 b)
Tin	232	2 622.8	$< 10^{-10}$	0.257	6 940 c)	15.08 b)	0.531 m)

1.5.1.1 Thermal conductivity

From the data in Table 1, it is easy to find that metals usually have much higher thermal conductivity than water whose thermal conductivity is 0.6 W/m-K. By comparison, the thermal conductivity of metals range from 8.34-86.9 W/m-K. The first three metals in the table, mercury, cesium and gallium can keep liquid state around the room temperature.

Liquid rubidium has an outstanding coolant but it is very expensive and reactive. Tin, lithium and indium are also excellent working fluids for heat transfer because of their high thermal conductivity and specific heat per unit volume. But the only difficulty is their relatively high melting points which are not proper for CPU chip cooling. Sodium and potassium is that they are reactive towards air and water and thus easily cause fire hazard. The low vapor pressure is also crucial if the working condition is a high vacuum environment. Mercury also has a high vapor pressure and is a toxic material. Gallium and Cesium have fairly acceptable melting points and thermal conductivity. Gallium is regarded as better than cesium because of its low working temperature range, higher specific heat per unit volume, lower vapor pressure at room temperature and less reactive nature. It also has additional feature of being nontoxic. Because of the merits presented above, gallium could be a promising coolant when used in forced convection.

1.5.1.2 Surface tension σ

The surface tension of water is 0.072 N/m, which is lower than all of liquid metals shown in table 1. This advantage of liquid metal makes it possible to avoid and reduce the leakage in cooling systems as much as possible. Hardy (1985) measured the surface tension of liquid gallium using the sessile drop technique with an Auger spectrometer [15]. The surface tension in mN/m decreased linearly with the increase of temperature and may be described as 708-0.66(T-29.8), where T has the unit of centigrade.

1.5.1.3 Heat capacity *c*

The heat capacity of water is 4200 J/(kg-K), and that of liquid gallium is 370 J/(kg-K). Although the heat capacity per kilogram of liquid gallium is much smaller than that of

water, the specific heat per unit volume is similar to that of water [14]. The specific heat per unit volume for water is 4,200 kJ/(m^3-K) and 2,158kJ/(m^3-K) for liquid gallium. This feature is another merit allowing liquid gallium to be an attractive coolant in chip cooling system.

1.5.1.4 Boiling temperature

The boiling points of many liquid metals are universally high, and this allows a low working pressure for the liquid metal as coolant at normal temperature. The low working pressure in the cooler system improves safety and reliability and simplifies the design and manufacturing of the system substantially. Thus it can make it easier to operate the equipment. What's more, due to its high boiling point, the working fluid can be guaranteed as a single phase fluid so as to avoid sudden changes of pressure while working which is desired for stable chip cooling process [14].

1.5.1.5 Sub-cooling point

Gallium can commonly be remained in a liquid state at a temperature much lower than room temperature because of its large sub-cooling point. Figure 1.10 demonstrates an experimentally tested typical curve of the gallium temperature transients during the cooling and heating process. It is easily found that gallium can keep liquid state even when the temperature is decreased to as low as 0.89°C during cooling procedure. Proper temperature difference between the solidifying point and melting point enables it an excellent coolant for convective cooling [14].

1.5.1.6 Viscosity

The viscosities of pure metal and alloys can be represented by the Arrhenius equation, which is shown in Eq. (1.1). The Arrhenius equation depicts the viscosity data of metallic melting temperature within a confined temperature range

$$\eta = A\exp\left(\frac{E_v}{RT}\right) \tag{1.1}$$

where E_v denotes the activation energy as an energy barrier for the movement of atoms in liquid metals; R is the gas constant; A is a constant and T is the absolute temperature of the metal samples. The activation energy of the viscous flow can be determined from the experimental values of dynamic viscosity. Zhou and Chen (2003) provided an overview of the viscosity of liquid metals [16]. It is described that the viscosity of liquid metal may be a barrier for flowing. However, the dynamic viscosity is not very high. The dynamic viscosity of water is 1.002mPa.s at 20℃, while that of liquid gallium is 1.2 mPa at 77℃ which is only a little bit greater [17].

1.5.2 Electromagnetic pump

In water cooling system, mechanical pumps and peristaltic pumps are generally be used to drive water. These kinds of pumps can also be used to circulate the liquid metal similar as in water cooling system. However there are some problems with these mechanical pumps when they are working in the liquid metal coolers. For example, because of the high density of liquid metal it is hard to drive them to flow. Moreover, some other issues also occur such as liquid metal embrittlement in peristaltic pumps, etc. There are

several special methods to drive liquid metals. The electromagnetic pump (EM pump also called MHD pump and MFD pump) is one of these alternatives.

The concept of EM pump was created first in the 1960's where it was applied to the nuclear industry to pump sodium without any mechanical power [18]. The EM pumps for zinc and later for aluminum were produced in the 1970's. Nowadays, different EM pump systems are broadly used in many applications which liquid metal is regarded as coolant such as extrusion millet casting, metal refinery for transporting molten metals, alloys production etc. Two different designs of electromagnetic pumps for molten pumps have been developed for decades: (1) direct current (DC) electromagnetic pump and (2) linear induction electromagnetic (AC) pump. In a general direct current EM pump, a channel flow of an electrically conducting fluid is surrounded by a permanent magnetic field orthogonally oriented to that flow. A direct electrical current is applied across the fluid at a right angle to the flow and at a right angle to the magnetic field. Therefore, producing an Ampere force which drives the fluid through the channel [18]. The Ampere force defines the intensity and direction of the force applied on the conductor fluid under the combined influence of the electric current and the magnetic field. The magnetic field and electric current can be controlled by two independent electric power [19].

Figure 1.11 shows the principle of operation of a DC EM pump, where a is the channel height of the pump, b is the channel width and c is the useful length. The direction of Ampere force can be determined by left-hand principle (The magnetic induction lines pass through the palm. The direction for four fingers is that for current and thumb points the direction of Ampere force). The intensity of Ampere force can be expressed as Eq (1.2)

$$F = BIL\sin\theta \tag{1.2}$$

where B is the magnetic strength, I is the electric current, L is the length of conductor fluid normal to the flowing direction in the magnetic field and Θ is the angle between the magnetic field and the current.

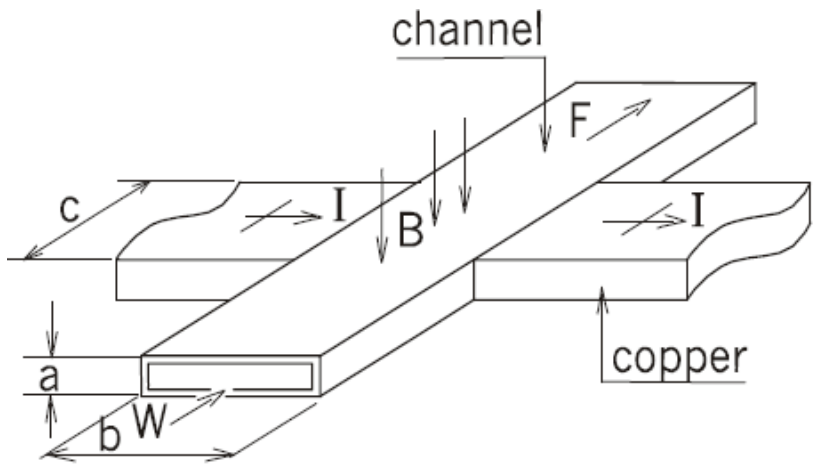

Figure 1.10. Working principle for a DC EM pump [19]

Because the liquid metal has high electrical conductivity, it can be driven by an EM pump which creates the Ampere force arising from the application of direct electric current normal to the magnetic field in the region of the fluid between two permanent magnets. The main advantages of EM pump lies in the ability to pump the working fluids efficiently with a silent, vibration free, low energy consumption rate without moving parts, and a compact geometry [14].

With obvious advanced over water cooling, liquid metal can be driven by an EM pump which includes non-moving parts, thus producing no noise and costs little power. In some special situations, the driving of a liquid metal can be done by the waste heat which means zero net energy input [20].

1.5.3 Applications and Practical Developments

Liquid metals have been applied on nuclear reactors as a kind of coolant for a long time. In 1963, the first nuclear powered submarine was launched which the liquid alloy of lead with bismuth is used as coolant [21]. Sato obtained an improvement of liquid metals through flow jet [22]. Up to now, using liquid metal for active cooling has been largely confined to nuclear powered plants. Liquid metal is also used in nuclear accelerators. Fast reactors generally use liquid metals as the primary coolant to cool the core and heat the water which is subsequently used to power electricity generating turbines. Except the nuclear power plant area, the liquid metals have already been used as a coolant in X-ray optics in high intensity synchrotron beam lines [23], mixed breeder blanket [24]. Because of its high electric conductivity, they are applied to reduce the electrical contact resistance as well [25]. From the numerous articles about liquid metal application, the technology has broad appeal for cooling nuclear reactors [26], electron thermalization process [27], etc.

As a newly emerging technology, the liquid metal used in CPU chip cooling is still in its early stages, and this kind of cooling device is still not commercially available. However, there are several researchers already started investigating this kind of devices and achieved some desired results. In 2002, Liu and his co-workers used liquid metal to demonstrate thermal management of a computer chip [10, 11]. After that, Miner and Ghoshal did further research to support his proposal in 2004 [12]. They considered the situation of hydrodynamically and thermally fully developed laminar and turbulent flows in a pipe of constant wall heat flux to demonstrate potential advantages of liquid metals over water. Analytical and experimental results show that heat transfer coefficient can be

generated on the order of 10W/cm^2-K and miniature EM pump operating at greater than 8kPa maximum pressure rise and 1% maximum efficiency. In 2005, a prototype of this newly proposed liquid metal chip cooling device is fabricated and the technical methods to build up this entire system were presented in Ref [28]. The schematic and prototype of the cooling devices are shown in Figure 1.12 (a) and (b).

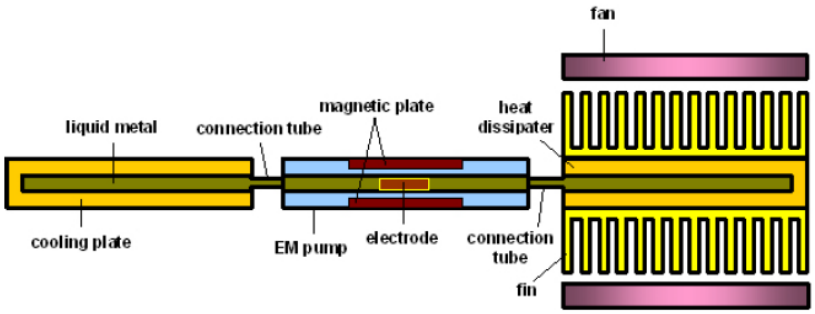

1.11. (a) Schematic of the cooling device with EM pump [28]

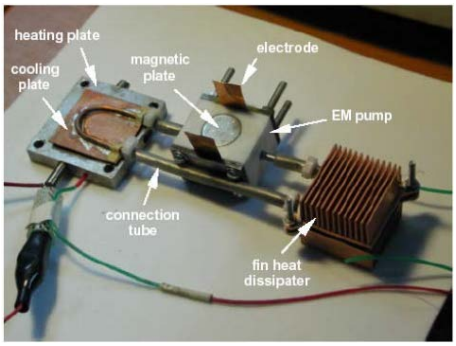

1.11. (b) Prototype of the cooling device with EM pump [28]

Liu and Li (2006) developed another system using liquid metal as coolant to reduce the temperature of electronic chips [29]. Numerous experiments under different flow rates and heat dissipation rates were conducted. The cooling performance of the liquid metal were compared with that of water cooling and good results were achieved. The temperature in the heated region almost immediately drops from its highest 70 °C to 46.7 °C when the

flow of liquid gallium was started. However, in the case of using water as coolant, the heating plate temperature only drops from 70 ℃ to 51.9 ℃. The results illustrated that the temperature of the CPU chip can be largely reduced with the increasing flow rate of liquid gallium which indicated that higher heat flux dissipation can be realized with a larger flow of liquid gallium and larger heat dissipation area. The prototype of the system is presented in Figure 1.12.

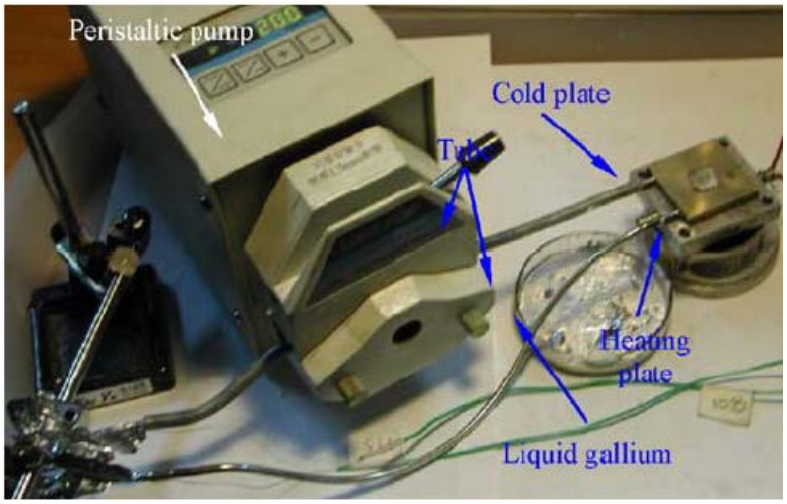

Figure 1.12. Prototype of liquid metal cooling device [29]

In order to make full use of the double advantages of liquid metal, Liu and Ma illustrated the liquid cooling concept for the thermal management of a CPU chip using waste heat to power the thermoelectric generator (TEG) and flow of the liquid metal [30]. This device requires no external energy which is self-supporting and completely silent. Experiments on systems driven by one or two stage TEGs demonstrated that a significant temperature drop on the chip has been achieved without the aid of fans. Moreover, the higher the heat load, the larger temperature decrease will be obtained by this cooling device.

The principle and prototype of liquid metal cooling system is shown in Figure 1.13 (a), (b) and (c).

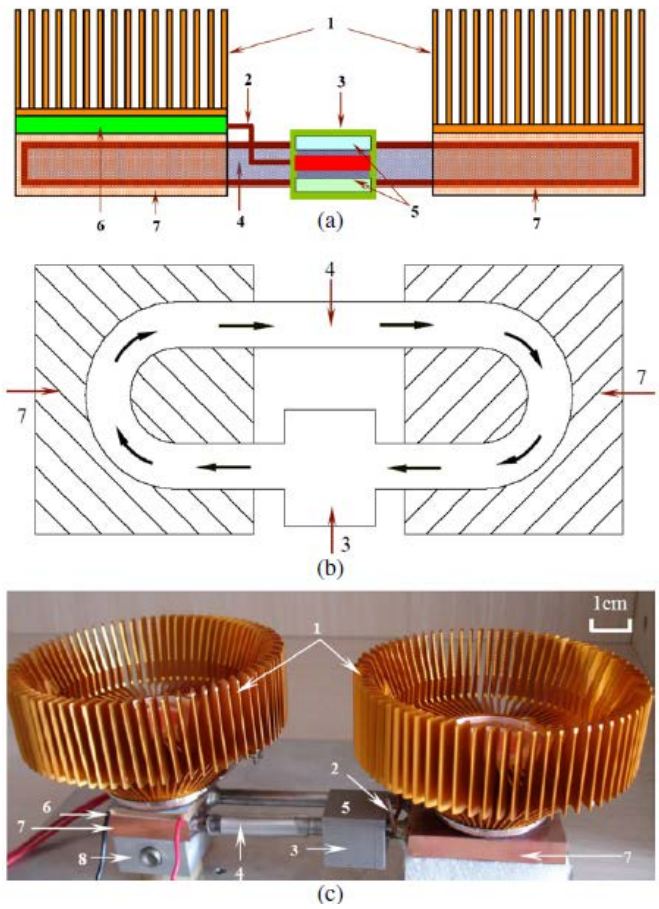

Figure 1.13. Principle and prototype of liquid metal cooling system driven by a TEG [30]. 1. Finned heat sink; 2. Electrodes of TEG; 3. EM pump; 4. Liquid metal; 5. Magnetic plate; 6. TEG; 7. Substrate with flow channels; 8. Simulating chip. (a) Principle, (b) top view of closed loop channel for liquid metal flow and (c) prototype.

Based on the results from previous thesis, Liu and Ma (2008) did further experiments to investigate the characteristic of this heat driven liquid metal chip cooling device under different power [31]. Experiments indicated that the temperature of chip can be kept under 90°C when the power is 50W. Additional, the higher power can result in a larger electric current generated by TEG and thus a stronger driving force.

Although liquid metal cooling devices have lots of advantages over water cooling systems, the relatively high cost of liquid metal is a significant disadvantage. In order to minimize the amount of the liquid metal used in the cooling device, a tower structure design was implemented which GaInSn alloy with melting point around 10℃ was selected to be coolant in 2010 [32]. Several critical design principles and fundamental theories were discussed first to better understand the design procedure. And in the experimental process, two typical prototypes which are shown in Figure 1.14 (a) and (b) have been manufactured to assess the cooling performance of this kind of cooling device. These results show that the liquid metal systems can represent outstanding cooling performance when compared with conventional water cooling system and heat pipes. The thermal resistance could be as low as 0.13℃/W, which is competitive with most of the commercial cooling devices in the market currently.

Figure 1.14 Two liquid metal cooling prototypes with (a) square and (b) flat structure [32]

The concept of liquid metal cooling discussed above is expected to provide a useful cooling strategy for the laptop, desktop and even larger computer. It can also be extended to broader area involved with thermal management on high heat flux [29]. High brightness light emitting diodes (LEDs) is quickly becoming a new generation of lighting

source for its many unique features, such as long life-span, lower energy consumption, environmentally friendly characteristics and so on [33]. However, because the junction temperature which should be remained below 120℃ had significant influence on the optical performance and reliability of LED [34], heat removal is still a big challenge for high power LEDs. In 2010 a LED cooling system with liquid metal as the coolant was proposed in Ref [35]. A series of experiments under different operation conditions were conducted to evaluate the cooling capability of the liquid metal cooling device, and the results were compared with that of water. The results indicated that liquid metal cooling system could have much higher cooling capability than that of a water cooling system. Meanwhile, a theoretical thermal resistance model was utilized to describe performance. Both the experiments and theoretical analysis demonstrated that liquid metal cooling system could have much better cooling performance than that of water. The higher convective heat transfer coefficient was the main reason for liquid metal to be an excellent coolant in cooling system. What's more, Liu and his research group applied this technique of liquid metal cooling on thermal management of Li-ion battery which is the heart of electric vehicles and can directly influence the working condition of the whole vehicle [36]. Mathematical analysis and numerical simulations are performed to evaluate the cooling performance, pump power consumption and module temperature uniformity of the liquid metal cooling device and compare it with that of water cooling system. The results demonstrated that under the same flow condition, liquid metal flow can realize a lower and more uniform temperature than water cooling with less pump power consumption and maintenance requirement. Moreover, liquid metal has an outstanding cooling performance

dealing with stressful situations, such as high power draw, defects in cells, and high ambient temperature.

1.6 Motivation of This Work

The advantages of using liquid metal for thermal management can be summarized as follows: 1) high cooling capability; 2) low thermal resistance; 3) single-phase fluid; 4) environmentally friendly; 5) compact and flexible configuration; 6) capable to cool multiple heat sources; 7) gravity-independence; 8) silent and highly reliable due to non-moving parts in EM pump. Based on these features, this work focused on the novel design of liquid metal heat sink for laptop computers. In order to better understand the design process, theoretical analysis for fluid flow and heat transfer performance of liquid metal and heat sink are conducted. Furthermore, in order to demonstrate the feasibility of this new concept, a series of experiments on the fabricated module under different heater powers and pump power are performed.

Chapter 2 Mathematical Analysis

2.1 Heat Sink Efficiency Evaluation

The conventional finned heat sink is used to improve the heat transfer rate from a heating surface by increasing the effective surface area. The working process involves heat transfer by conduction within a solid fin and by convection from the boundaries of the solid to surrounding fluid such as, air. A heat sink is comprised of numerous fins, so a complete thermal analysis must consider the combined effect of all fins and regions of the heat sink between fins. Air flow is forced over the fins of the heat sink using a fan, transferring heat from the fin surface to the air via convection.

2.1.1 Single Fin Efficiency Evaluation

The simplest case of straight rectangular fins of uniform cross section is applied in this experiment and the configuration is shown in Figure 2.1.

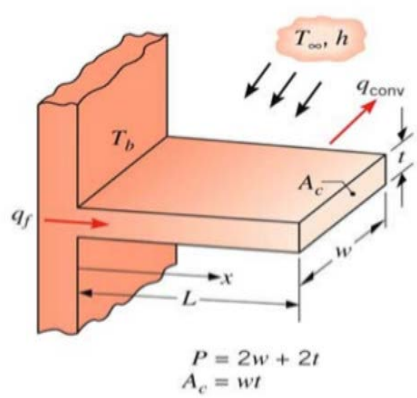

Figure 2.1. Configuration of rectangular fin [37]

A definition of excess temperature θ is introduced as

$$\theta(x) = T(x) - T\infty \tag{2.1}$$

where T(x) is the temperature at x point on the fin and T_∞ is the ambient air temperature.

Fin performance is provided by fin efficiency η_f. The maximum driving potential for convection is the temperature difference between the fin base (x=0) and the fluid, $\theta_b = T_b - T_\infty$. The maximum heat transfer rate would exist under the condition of assuming the entire fin surface are at the same base temperature. The definition of fin efficiency is shown below

$$\eta_f = \frac{q_f}{q_{\max}} = \frac{q_f}{hA_f\theta_b} \tag{2.2}$$

Where q_f is the fin heat transfer rate which will be shown in Table 2.1 and A_f is the surface area of the fin.

Table 2.1. Temperature distribution and heat loss for fins with uniform cross section [37]

Case	Tip Condition ($x = L$)	Temperature Distribution θ/θ_b	Fin Heat Transfer Rate q_f
A	Convection heat transfer: $h\theta(L) = -kd\theta/dx\|_{x=L}$	$\frac{\cosh m(L-x) + (h/mk)\sinh m(L-x)}{\cosh mL + (h/mk)\sinh mL}$	$M\frac{\sinh mL + (h/mk)\cosh mL}{\cosh mL + (h/mk)\sinh mL}$
B	Adiabatic $d\theta/dx\|_{x=L} = 0$	$\frac{\cosh m(L-x)}{\cosh mL}$	$M \tanh mL$
C	Prescribed temperature: $\theta(L) = \theta_L$	$\frac{(\theta_L/\theta_b)\sinh mx + \sinh m(L-x)}{\sinh mL}$	$M\frac{(\cosh mL - \theta_L/\theta_b)}{\sinh mL}$
D	Infinite fin ($L \to \infty$): $\theta(L) = 0$	e^{-mx}	M

$\theta \equiv T - T_\infty$ $\quad m^2 \equiv hP/kA_c$

$\theta_b = \theta(0) = T_b - T_\infty$ $\quad M \equiv \sqrt{hPkA_c}\theta_b$

Assuming under the case B in Table 2.1 (an adiabatic fin tip), substitute q_f into Equation 2.2 yields,

$$\eta_f = \frac{M \tanh mL}{hPL\theta_b} = \frac{\tanh mL}{mL} \tag{2.3}$$

where P is the perimeter of the cross section, L is the length of fin and m is a constant for specific fin.

2.1.2 Overall Surface Efficiency Evaluation

The fin efficiency η_f represents the performance of a single fin. However, the overall surface efficiency η_0 characterizes an array of fins and the base surface to which they are attached. The configuration of array is shown in Figure 2.2.

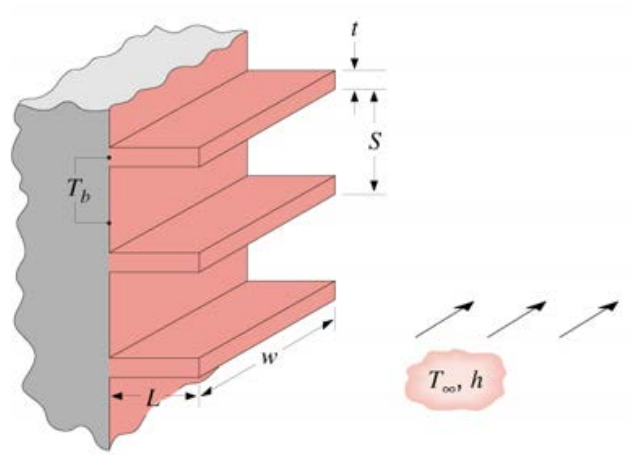

Figure 2.2. Representative fin arrays [37]

Where S is the gap between two fins. The overall efficiency is defined as

$$\eta_0 = \frac{q_t}{q_{\max}} = \frac{q_t}{hA_t\theta_b} \quad . \tag{2.4}$$

where q_t is the total heat transfer rate from the total surface area, A_t, which contains both the fins and exposed portion of the base. If there are N fins in the array, each surface area is A_f, and the unfinned surface area is A_b, the total surface area is

$$A_t = NA_f + A_b \tag{2.5}$$

The total convection heat transfer rate can then be expressed as

$$q_t = N\eta_f hA_f\theta_b + hA_b\theta_b \tag{2.6}$$

where the convection coefficient, *h*, is assumed constant for the entire surface. Hence,

$$q_t = h[N\eta_f A_f + (A_t - NA_f)]\theta_b = hA_t[1 - \frac{NA_f}{A_t}(1-\eta_f)]\theta_b \tag{2.7}$$

Substituting Equation 2.9 into 2.6 yields,

$$\eta_0 = 1 - \frac{NA_f}{A_t}(1-\eta_f) \tag{2.8}$$

Fins performance can also be assessed in terms of thermal resistance. Recalling the definition of thermal resistance, the thermal resistance of a fin array is

$$R_{t,0} = \frac{\theta_b}{q_t} = \frac{1}{\eta_0 hA_t} \tag{2.9}$$

2.1.3 Convection Heat Transfer Coefficient Calculation

In order to estimate the heat sink performance, calculation of the convection heat transfer coefficient is an initial task. The configuration of the heat sink in this experimental set up is shown in Figure 2.3 (a) and (b).

(a)

(b)

Figure 2.3 Configuration of heat sink (a) cross-sectional view (b) top view

The parameters of the heat sink is summarized in Table 2.2.

Table 2.2. Parameters of the heat sink. Refer to Figure 2.2.

L(m)	1.2×10^{-2}
W (m)	3.55×10^{-2}
t (m)	3.45×10^{-4}
S (m)	1×10^{-3}
N	58
k_{copper} (W/m.K)	401

And the thermal physics properties of air is shown in Table 2.3.

Table 2.3 Thermal physics properties of air

T(K)	300
ρ (kg/m^3)	1.1614
Cp (kJ/kg.K)	1.007
μ (N.s/m^2)	184.6×10^{-7}
ν (m^2/s)	15.89×10^{-6}
k_{air} (W/m.K)	26.3×10^{-3}
Pr	0.707

For internal flow of non-circular tube, many of the results may be applied by using a hydraulic diameter as the characteristic length and it is defined as

$$D_h = \frac{4S \times L}{2(S+L)} = \frac{4A_s}{P_s} \tag{2.10}$$

The value of hydraulic diameter for the area between adjacent fins is 1.84×10^{-3}m. Assuming a total volumetric flow rate is 10 cubic feet per minute (0.00472 m^3/s) is generated by the fan, the value of mass flow rate $\dot{m}$ is 5.4×10^{-3}kg/s and 9.47×10^{-5}kg/s per channel by equation $\dot{m} = \rho.\dot{V}$. When dealing with the internal flows, it is important to judge whether the flow is laminar or turbulent. The Reynolds number is defined as

$$\mathrm{Re}_{D_h} = \frac{\rho u_m D_h}{\mu} = \frac{\dot{m} D_h}{A_s \mu} \tag{2.11}$$

Where μ is the dynamic viscosity. Substitute the value of this parameters into the equation 2.11, the Reynolds number is 789.614 which is less than the critical Reynolds number value of 2300. Therefore, this internal flow is laminar flow.

Since the condition of laminar flow is decided, next emphasis is placed on determining the Nusselt number of the airflow between fins. Check the table 2.4 [37] under uniform surface temperature (as a conservative estimate), the Nusselt number in this condition is 5.6. From the equation 2.12 shown below,

$$h = \frac{Nu_D K}{D_h} \tag{2.12}$$

The convection heat transfer coefficient calculated is 79.77W/m^2K.

Table 2.4. Nusselt Number and friction factor for fully developed laminar flow in differing cross section [37]

Cross Section	$\frac{b}{a}$	$Nu_D = \frac{hD_h}{k}$ (Uniform q''_s)	$Nu_D = \frac{hD_h}{k}$ (Uniform T_s)	$f\,Re_{D_h}$
	—	4.36	3.66	64
	1.0	3.61	2.98	57
	1.43	3.73	3.08	59
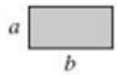	2.0	4.12	3.39	62
	3.0	4.79	3.96	69
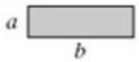	4.0	5.33	4.44	73
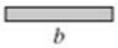	8.0	6.49	5.60	82
	∞	8.23	7.54	96
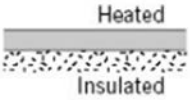	∞	5.39	4.86	96

2.1.4 Results

Substitute the heat transfer coefficient calculated above and other value into equation 2.5, the efficiency of single fin with convection tip is 94.8%. From equation 2.8 and 2.9, the final overall surface efficiency is 97.5%, and the overall thermal resistance is 0.12 ℃/W.

2.2 Channel Flow Analysis

2.2.1 Internal Flow Convection Heat Transfer Coefficient Calculation

The input voltage and current for electromagnectic pump is V and I measured by multimeter, respectively. Therefore, the input power for pump is

$$P = V \times I \tag{2.13}$$

According to the equation 1.2 and figure 1.11, the electromagnetic force is expressed as

$$F = BIb \tag{2.14}$$

Where B is the magnetic field intensity (Tesla) and b is the width of the channel. Thus it is easily to obtain the equation of the pump head (force divided by cross-sectional area)

$$\Delta p = \frac{F}{ab} = \frac{BI}{a} \tag{2.15}$$

From the relation between the input power and volumetric flow rate $P = \frac{\Delta p . Q_v}{\eta}$, the liquid metal flow rate can be expressed as

$$u_m^{'} = \frac{V}{Bb} \tag{2.16}$$

The parameters for electromagnetic pump and channel are shown in Table 2.5

Table 2.5 electromagnetic pump and channel related parameters

Input voltage V (V)	0.25
Input current I (A)	11.22
Magnetic field intensity B (T)	0.9 (estimated)
Channel height a (m)	2×10^{-3}

Channel width b (m)	12×10^{-3}
Channel length L (m)	0.704
Efficiency η	0.1% (estimated)

Substitute the value into equation 2.16, the liquid metal flow rate is 0.023 m/s.

For the estimation of the magnetic field intensity, information about permanent magnet values from Wikipedia is referenced, and shown in Table 2.6 . A value of 0.9 T was selected. Regarding the estimation of the pump efficiency, the experimental data was applied to this equation,

$$P = \rho C_P u_m A_c (\overline{T}_{fout} - \overline{T}_{fin}) \tag{2.17}$$

Where P is the power of the heater, ρ and C_p is the density and heat capacity of liquid gallium alloy, u_m is the liquid gallium flow rate and A_c is the cross section area of the channel. After applying the temperature difference into equation (2.17), the value of u_m can be obtained. Going back to $P = \frac{\Delta p.Q_v}{\eta}$, the pump efficiency is approximately 0.1%.

Table 2.6 Calculated the measured magnetic field [19].

Magnet	B_r (T)	H_{ci} (kA/m)	BH_{max} (kJ/m^3)	T_C	
				(°C)	(°F)
$Nd_2Fe_{14}B$ (sintered)	1.0–1.4	750–2000	200–440	310–400	590–752
$Nd_2Fe_{14}B$ (bonded)	0.6–0.7	600–1200	60–100	310–400	590–752
$SmCo_5$ (sintered)	0.8–1.1	600–2000	120–200	720	1328
$Sm(Co, Fe, Cu, Zr)_7$ (sintered)	0.9–1.15	450–1300	150–240	800	1472
Alnico (sintered)	0.6–1.4	275	10–88	700–860	1292–1580
Sr-ferrite (sintered)	0.2–0.78	100–300	10–40	450	842

Similar with the process for calculating the convection heat transfer coefficient for heat sink, obtaining the hydraulic diameter for flow channel is an initial task because of the noncircular cross section,

$$D_h^{'} = \frac{4A_c^{'}}{P^{'}} \tag{2.18}$$

The value for this hydraulic diameter is 0.00342 m. When dealing with the internal gallium flow, it is important to judge whether the flow is laminar or turbulent. The Reynolds number is defined as

$$\mathrm{Re}_D^{'} = \frac{\rho^{'} u_m D_h^{'}}{\mu^{'}} \tag{2.19}$$

The thermal physical properties of gallium are illustrated in table 2.7

Table 2.7 Thermal physical properties of liquid gallium

Density ρ (kg/m^3)	6263
Dynamic viscosity μ (N.s/m^2)	0.002
Thermal conductivity *K* (W/m.K)	30
Prandlt number *Pr*	0.0208
Heat capacity *Cp* (J/kg.K)	500

Substituting the values shown above into equation 2.19, the Reynolds number obtained is 246.32 which is less than the critical value of 2300. Hence, the condition of the channel flow is laminar. According to table 2.4 [37], the corresponding Nusselt number is 5.33. Applying the same equation 2.12, the convection heat transfer coefficient is 46,754 W/m^2. K.

2.2.2 Pressure Drop Calculation

Pressure drop is defined as the difference in pressure between two points of a fluid carrying network. It occurs when frictional forces, caused by the resistance to flow, act on a fluid as it flows through the tube. In order to calculate the pressure drop for the whole channel loop, it is necessary to start with Moody friction factor which is expressed as

$$f = \frac{-(dp/dx)D_h^{'}}{\rho^{'} u_m^{2'}/2} \tag{2.20}$$

So the equation for pressure drop can be obtained

$$\Delta p^{'} = -\int_{p_1}^{p_2} dp = f^{'} \frac{\rho^{'} u_m^{2'}}{2D_h^{'}}(x_2 - x_1) = f \frac{\rho^{'} u_m^{2'}}{2D_h^{'}} L \tag{2.21}$$

Where $f = \frac{73}{\mathrm{Re}_D}$ in laminar flow. Substituting the value of parameters into equation (2.21), finally, the value of pressure drop is 102.3 Pa, which is less than the pump head (5049 Pa).

Chapter 3 Experimental System and Procedure

This chapter gives a brief introduction for the prototype, experimental set-up, and procedure in order to better understand the cooling performance of this set-up, which will be discussed in next chapter.

3.1 Prototype

The whole prototype is a simulating internal structure of laptop consisting of heaters representing “CPU chip”, “hard drive” and “graphic processor” is shown in Figure 3.1(a) and 3.1(b). The material of the heater is copper and surface area is 405 mm^2.

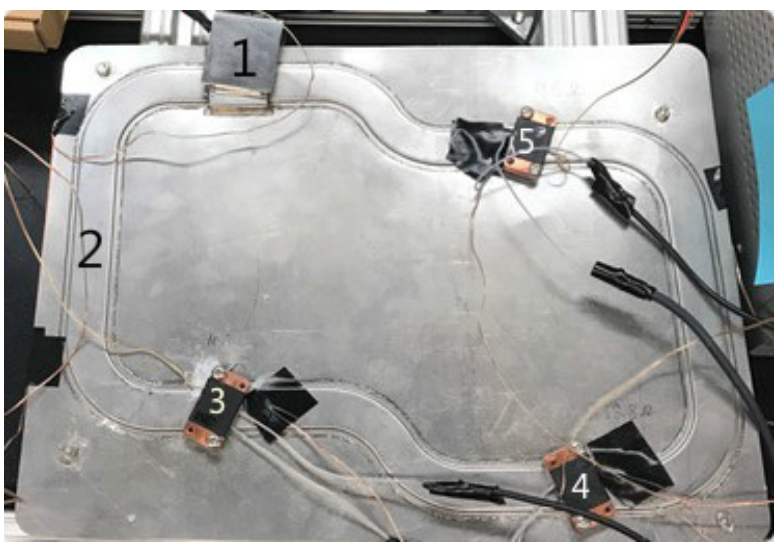

Figure 3.1. (a) Prototype front side. 1. Electromagnetic pump; 2. Flow channel; Resistive heaters representing 3. Hard drive; 4. Graphic processor; 5. CPU chip

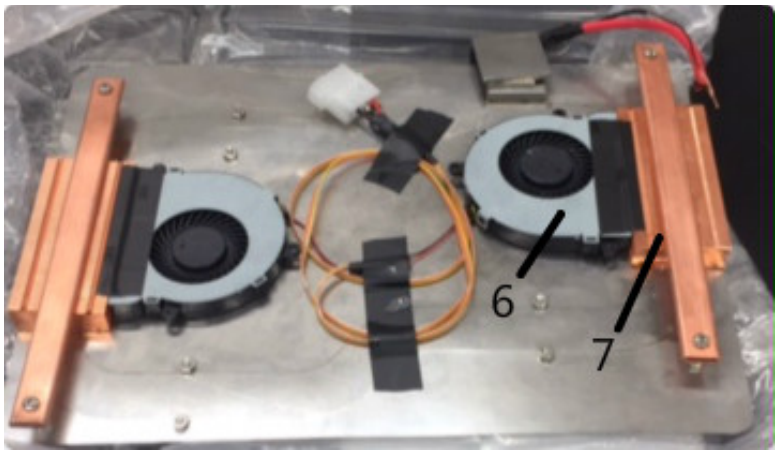

Figure 3.1. (b) Prototype back side. 6. Fans; 7. Heat sink

The length and width of the prototype is 269mm and 203mm, respectively. The liquid gallium flow channel is underneath the heaters and is driven by the electromagnetic pump described before. The fans on the backside are used to create forced airflow across copper heat sinks for heat rejection. Each fan generates 10 cfm of forced airflow across the heat sink.

3.2 Thermocouple Distribution

For electronic cooling experiments, the application of the thermocouples is of vital importance. In this test, K-type thermocouples are applied and its distribution are presented in Figure 3.2 (a) and (b). The thermocouples were applied by epoxy and several layers of the tape to secure them to the channel. Because of the very high internal thermal convection coefficient provided by the liquid metal flow, the temperature measured on the external surface of the channel is assumed to be nearly equal to that of the liquid metal underneath.

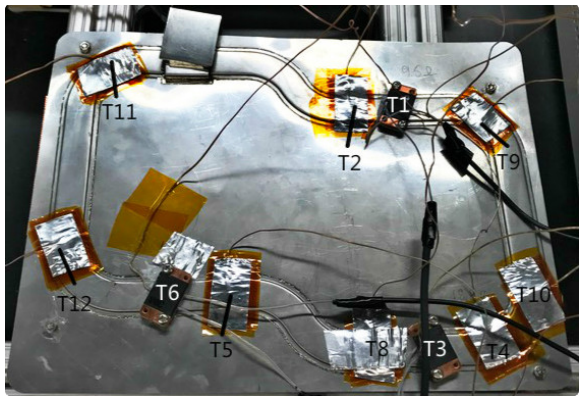

(a)

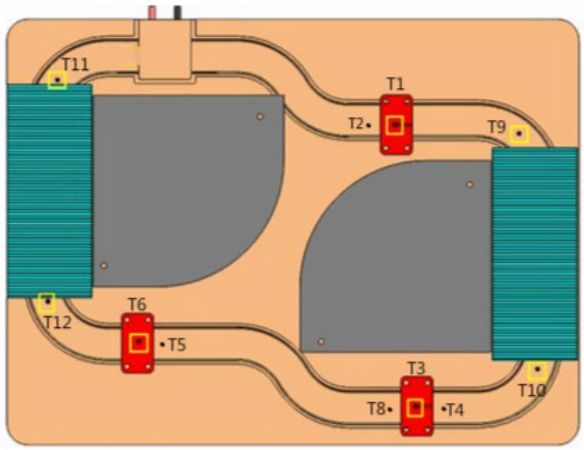

(b)

Figure 3.2. Configuration of thermocouples distribution (T1-T11 represent the location of thermocouples)

3.3 Experimental Setup

The whole experimental setup is shown in Figure 3.3.

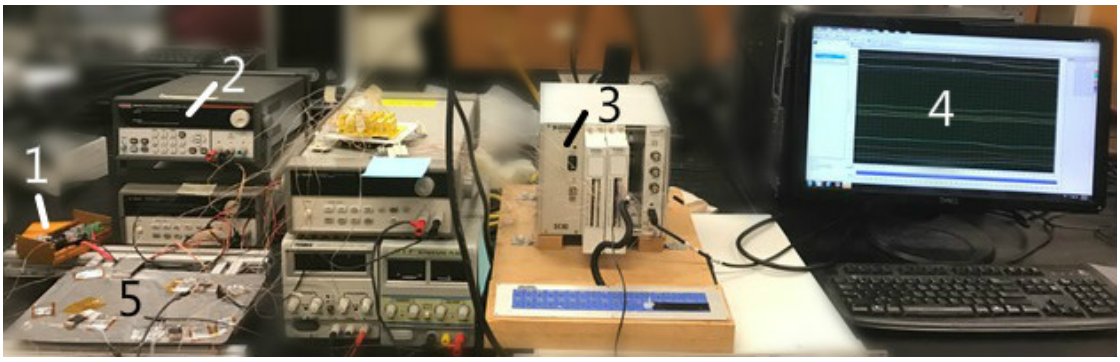

Figure 3.3. Experimental Setup. 1. DC Transformer; 2. DC Power 3. Data Acquisition Control Unit; 4. Personal Computer with Labview Software 5. Prototype

There are five DC power supplies in total to power three resistance heaters, fans and DC transformer. The make and model of the DC powers is Agilent E3604A, TENMA 72-6610, WEB PS-305D and KEITHLEY 2200-60-2. The model of DAQ is National Instruments SCXI-1000.

A DC transformer is shown in Figure 3.4 to convert a high voltage and low current to low voltage and high current. As shown later, the electrical current output from the transformed exceeded 10 A.

Figure 3.4. Voltage Transformer

3.4 Experimental Procedure

The detailed procedure can be summarized as follows:

1. Turn on the DC power for fans and the voltage transformer to drive the electromagnetic pump. The voltage for fans and pump transformer is 5V and 12V, respectively.

2. If under the insulation condition, put some fiber glass above the prototype.

3. Record thermocouple data using labview software.

4. Switch on the DC power for CPU chip, hard drive and graphic processor and adjust the power to approximately 5W, 10W, 15W and 20W.

5. Monitor the temperature telemetry data. When the temperature reaches the steady state (+/- 0.1 per minute), stop recording and save data. After obtaining each set of data, adjust the total input power for heaters by 5W and repeat the same procedure listed above. A period of approximately 30 minutes was necessary to achieve steady state. During the test process, the input power and temperature data were recorded through the data acquisition unit.

Chapter 4 Results and Discussions

The ambient room temperature was measured at 25℃ +/- 1℃. In the experiment, the temperatures of heaters surface and the temperature of the channel before and after the heaters or heat sinks are measured by multiple K-type thermocouples, with results shown in Figure 3.2. To find out the input energy the electromagnetic pump consumes, corresponding parameters including the voltage and electric current were measured by multimeter. The flow direction of the liquid gallium is clockwise on the front side. In addition, the related parameters of the fan and pump are demonstrated in Table 4.1.

Table 4.1 Related parameters of the fans and pump

Room Temperature		25℃
Pump Parameters	Dimensions	20mm×15mm×8mm
	Voltage(V)	0.25
	Current(I)	11.22
Fan Parameters	Dimensions	Φ60mm×8.0mm
	Voltage(V)	5.0
	Current(I)	0.8

4.1 Heater Power Influence

Figure 4.1 shows the steady-state temperature profile at different points around the channel loop under different heater powers without (a) or with insulation (b). The tested data is shown in Table 4.2 (a), (b).

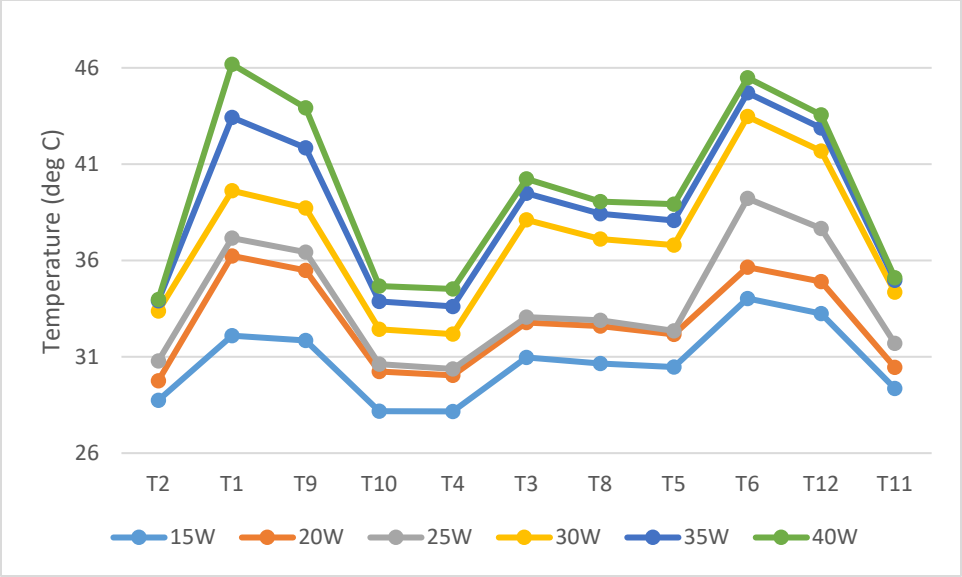

(a)

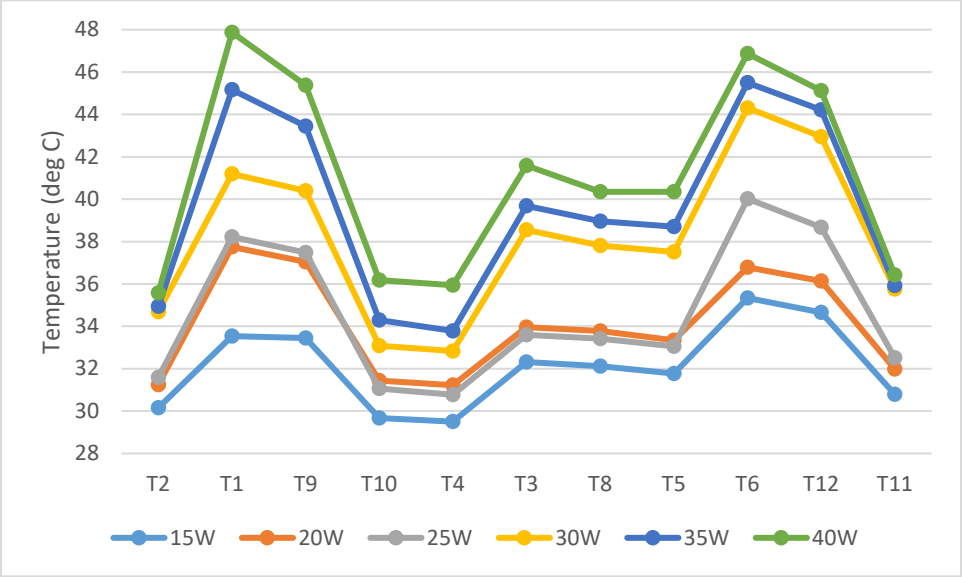

(b)

Figure 4.1. Steady state temperature under different power (a) without insulation (b) with insulation

When the liquid gallium flows through the heater, it absorbs the heat and results in temperature increase (T9>T2, T8>T4, T12>T5). The heat sinks and fans reject the heat from the channel to ambient air leading to temperature decrease. Under the insulation

condition, the final temperature was several degrees higher than that without insulation because parasitic heat loss from the stainless steel prototype board is suppressed. Table 4.1 lists the steady state temperature measurements for each set of power conditions.

Table 4.2 (a). Experimental data under different power without insulation

	T2	T1	T9	T10	T4	T3	T8	T5	T6	T12	T11
15W	28.74	32.09	31.84	28.17	28.17	30.97	30.65	30.47	34.03	33.25	29.36
20W	29.76	36.24	35.48	30.23	30.03	32.78	32.59	32.16	35.65	34.90	30.45
25W	30.79	37.16	36.44	30.62	30.37	33.06	32.90	32.35	39.22	37.66	31.69
30W	33.38	39.61	38.73	32.42	32.18	38.11	37.12	36.80	43.47	41.69	34.35
35W	33.91	43.43	41.84	33.87	33.62	39.48	38.42	38.08	44.70	42.87	34.98
40W	33.97	46.19	43.92	34.67	34.52	40.25	39.05	38.93	45.49	43.57	35.10

Table 4.2 (b). Experimental data under different power with insulation

	T2	T1	T9	T10	T4	T3	T8	T5	T6	T12	T11
15W	30.16	33.54	33.45	29.67	29.50	32.32	32.12	31.78	35.34	34.65	30.79
20W	31.25	37.75	37.03	31.44	31.22	33.96	33.77	33.34	36.78	36.14	31.99
25W	31.59	38.22	37.47	31.05	30.77	33.60	33.41	33.05	40.02	38.67	32.51
30W	34.69	41.20	40.39	33.09	32.83	38.55	37.81	37.52	44.31	42.95	35.75
35W	34.95	45.17	43.44	34.30	33.78	39.68	38.96	38.70	45.49	44.21	35.93
40W	35.58	47.87	45.37	36.19	35.94	41.59	40.35	40.35	46.87	45.12	36.42

Figure 4.2 (a), (b) demonstrate the steady state temperature variation trend as a function of input power. Higher heater power leads to an increase in temperature at all locations, as expected. After the total heater power (summation of all heat loads) exceeds 30W, the slope of temperature with increased power decreases. Even when the total heater power is 40W, the steady state temperature is still under 50 ℃. The thermal resistance for

both overall system and heat sink is approximately in the range of 0.4-0.5 °C/W. The thermal resistance for heat pipe cooling system [1] is in the range of 0.4-0.6 °C/W. The minimum thermal resistance for oscillating heat pipe [7] is approximately 0.32 °C/W. For water cooling system, the thermal resistance is around 0.1 °C/W for desktop. Therefore, the performance of this system is modest and slightly less efficient than existing technologies.

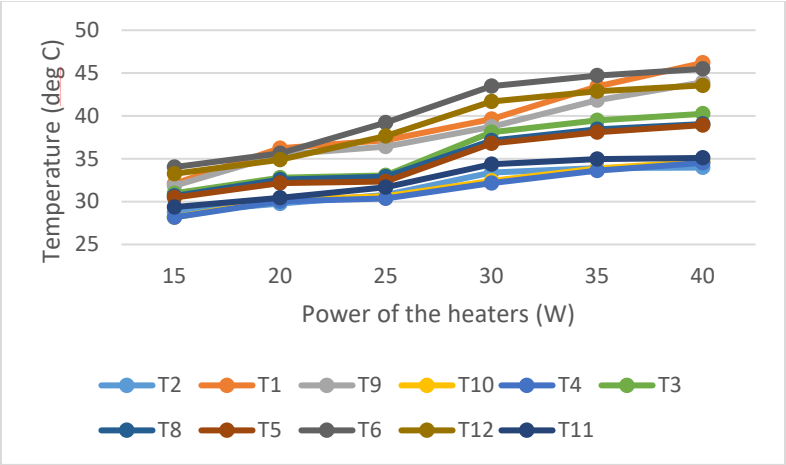

(a)

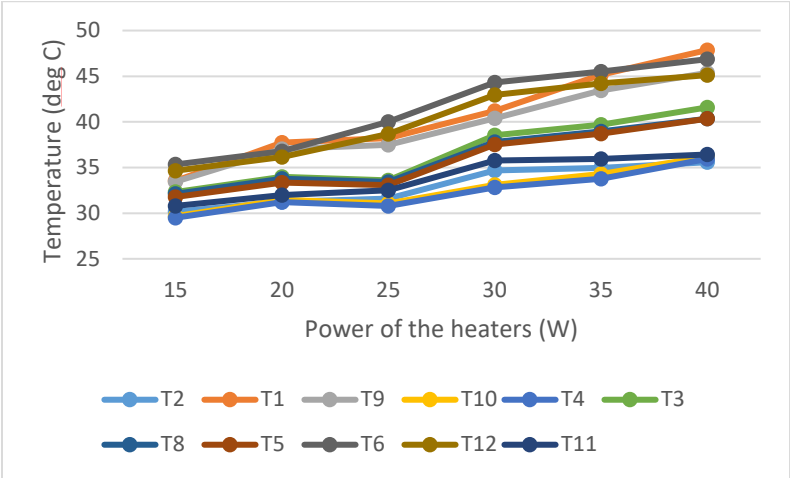

(b)

Figure 4.2. Steady state temperature variation tendency with power increasing (a) without insulation (b) with insulation

4.2 Pump Power Influence

The electromagnetic pump required a minimum power to begin circulation of gallium. The minimum power was found to be 1.474 W (the input voltage of 0.22 V and current of 6.7 A). This condition restricts the operation conditions in which the pump may operate. Nevertheless, the cooling performance at this lower power conditions was considered. The comparison results are shown in Figure 4.3 and Table 4.3 under the circumstance of heaters power are 40 W without insulation.

Table 4.3 Comparison results under 40 W heater power

Temperature (°C)											
Pump power (W)	T2	T1	T9	T10	T4	T3	T8	T5	T6	T12	T11
1.474	34.60	47.96	45.76	35.64	35.54	42.02	40.73	40.69	48.05	46.15	35.66
2.805	33.97	46.19	43.92	34.67	34.52	40.25	39.05	38.93	45.49	43.57	35.10

Figure 4.3. Comparison results between low pump power and regular pump power

The mass flow rate of the gallium may be obtained by evaluating the temperature increase across resistance heaters using equation 2.17. Assuming that all heater energy is absorbed by the flowing gallium, the mass flow rate may be determined. Based on this process, the mass flow rate is 0.004 kg/s +/- 0.0004 kg/s. Based on this mass flow rate, we can estimate the pump efficiency as 0.1 %, consistent with previous findings [38].

4.3 Comparison Between Theoretical and Experimental Results

According to the equation (2.17), a simulation was performed by using experimentally-extracted performance metrics. The temperature of the fluid existing the pump, T2, was extracted from experimental data. Each of the two heat sinks were assumed to feature the same thermal resistance because of their identical design. Further, the total heat rejected by the two heat sinks must be equal to the heat absorbed by the gallium from the heaters. All heat produced by the heating elements was, likewise, assumed to be absorbed by the gallium. The temperature profile was solved iteratively because the heat rejection rate from either heat sink was not known explicitly. The solution converged when the total heat rejected by both heat sinks summed to equal the heat input from the resistance heaters. The comparison between the modeled and experimental results are shown in Figure 4.4. Note that the model does not consider heat loss from the prototype board. Based on the model, the thermal resistance of each heat sink is 0.84 °C/W in comparison to the theoretical value of 0.12 °C/W previously computed. The difference is attributed, in part, to thermal contact resistance between each heat sink and the flow channel. Furthermore, the 10 gpm assumed flow rate produced by each cooling fan may be an overestimate, as

pressure losses through the narrow heat sink flow channels may greatly restrict the airflow rate in the given application.

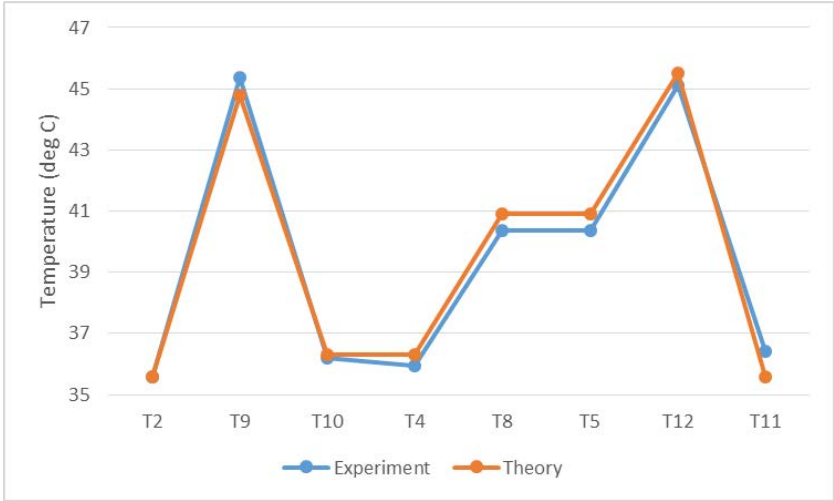

Figure 4.4. Comparison between theoretical and experimental results

4.4 Coefficient of Performance

The coefficient of performance (COP) is another important metric to consider when characterizing the liquid metal heat sink. The COP is defined as the useful cooling provided by the system divided by the power consumed by the system. In the current system, power is consumed to drive 2 fans and the electromagnetic liquid gallium pump. Based on a heat rejection rate of 40W, a pump power of 2.8W, and a combined fan power of 4W the COP for the liquid metal heat sink is approximately 0.3.

Chapter 5 Conclusions

5.1 Summary and Conclusions

According to the experimental data, the maximum component temperature is lower than 50 ℃ under 40W of total heat load, resulting in an overall thermal resistance that is in the range of 0.5-0.6 ℃/W. This value is similar with that of heat pipe heat sinks (0.4-0.6 ℃/W), oscillating heat pipes (minimum is 0.32 ℃/W). Furthermore, the large thermal resistance of the heat sinks was unexpectedly high and could be further enhanced by reducing thermal contact resistance and increasing force airflow. Perhaps the largest bottleneck of performance is experienced by the liquid metal pump.

With a pumping efficiency of only 0.1%, the pump draws an unacceptable amount of electrical energy. An increase in pumping efficiency would directly increase the mass flow rate of gallium, which would in turn decrease the temperature increase across components. To estimate the performance of a system with doubled pump efficiency, the simulations from the previous chapter was run with double the gallium mass flow rate and the same heat sink resistance values. The results in Figure 5.1 shows that the maximum temperature decreases by only 1.5℃.

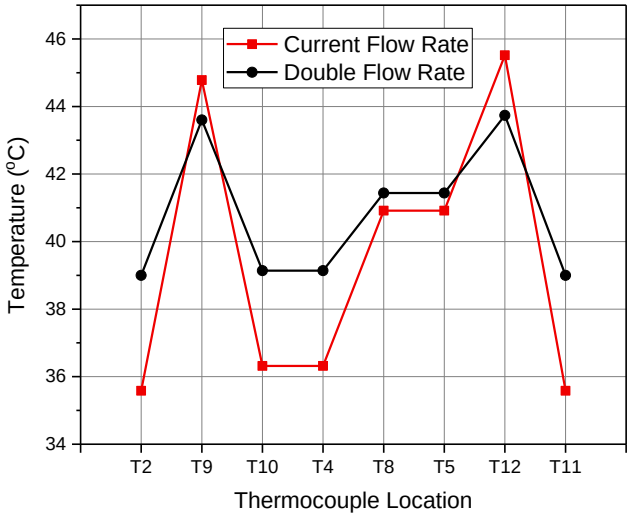

Figure 5.1. Simulated temperature profile with double gallium mass flow rate.

Next, the thermal resistance of the heat sinks was addressed by assuming a decrease in thermal resistance by a factor of 2. Notice that reducing the heat sink resistance resulted in a temperature decrease of between 7-9°C for all locations, suggesting that addressing the heat sink resistance could have greater impact on reducing thermal resistance than increasing the pump power. Further investigation in this area is suggested.

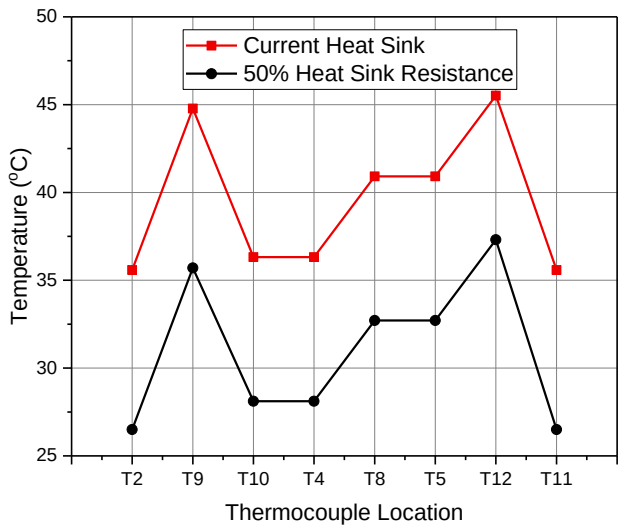

Figure 5.2. Simulated temperature profile with heat sinks having 50% thermal resistance of the current heat sinks.

5.2 Future Work

From the results shown above, the performance of this novel liquid metal cooling system is outstanding compared with other cooling systems. However, more work can also be put on this research to gain greater performance. The efficiency of the electromagnetic pump in this prototype is is only 0.1 %. Improving the performance of the electromagnetic pump can be realized by reducing air gap, using higher magnetic field strength material, increasing the pump duct width, and reducing slip velocity. Applying more and larger heat sinks or more powerful fans is also an effective way to enhance the performance. However, noise level, size and other factors also need be taken into consideration. Moreover, modifying the shape or dimension of the channel loop could advance the performance of this liquid metal cooling system further. This phenomena indicates that liquid metal may be a viable cooling solution for laptop thermal management.

References

[1] Kim, K. S, Won, M. H, Kim, J. W, Back, B. J, 2003, “Heat pipe cooling technology for desktop PC CPU,” Applied Thermal Engineering, 23, pp. 1137-1144.

[2] Maydanik, Y. F, Vershinin, S. V, Korukov, M. A and Ochterbeck, J. M, 2005, “Miniature Loop Heat Pipes----A Promising Means for Cooling Electronics,” IEEE Transactions On Components And Packaging Technologies, 28, no. 2.

[3] Pastukhov, V. G, Maidanik, Y. F, Vershinin, C. V and Korukov, M. A, 2003, “Miniature loop heat pipes for electronic cooling,” Applied Thermal Engineering, 23, pp. 1125-1135.

[4] Albert W. Davis, Jr. Structure of a heat pipe. U. S. Patent 4, 921, 041, May 1, 1990.

[5] Albert W. Davis, Jr. Structure of a micro-heat pipe. U. S. Patent 5, 219, 020, June 15, 1993.

[6] Leonard L. Vasiliev, 2005, “Heat pipes in modern heat exchangers,” Applied Thermal Engineering, 25, pp. 1-19.

[7] Yury. F M, Valery I. D, Vladimir G. Pastukhov, 2009, “Compact cooler for electronics on the basis of a pulsating heat pipe,” Applied Thermal Engineering, 29, pp. 3511-3517.

[8] S. Rittidech, A. Boonyaem and P. Tipnet, 2005, “CPU cooling of desktop PC by Closed-end oscillating heat pipe.” American Journal of Applied Sciences, 12, pp.1574-1577.

[9] Zeng P, Cheng G M, Liu J L, Yang Z G, Zheng L B, 2005, “Compositive Water-Cooling System Applied to Computer Chip.” Journal Of Xi’An Jiao Tong University, 11, pp. 1207-04.

[10] Liu J, Zhou Y X, 2002, China Patent, No 021314195.

[11] Liu J, Zhou Y X, Lv Y G, Li T, 2005, ASME Int. Mech. Eng. Cong. & Exp, 501

[12] A Miner, U Ghoshal, 2004, “Cooling of high-power-density microdevices using liquid metal coolants.” Applied Physics Letters, 3, vol. 85.

[13] Sawada T, Naetchaev A, Ninokata H, 2000, “Gallium-cooled liquid metallic-fueld fast reactor,” Prog Nucl Energ, 37, pp. 313-319.

[14] Ma K Q, Liu J, 2007, “Liquid metal cooling in thermal management of computer chips.” Energy Power Eng, 4, pp. 384-402.

[15] Hardy S C, 1985, “The surface tension of liquid gallium.” J Cryst Growth, 7, pp. 602-606.

[16] Zhou X W, Chen J Y, 2003, “Overview on viscosity of liquid metals.” Journal of Shenyang Normal university, 21(4), pp. 255-259 (in Chinese).

[17] Prokhorenko S V, 2005, “Structure and viscosity of gallium, indium and tin in the vincinity of the crystallization temperature,” Materials Science, 41, pp. 271-274.

[18] Kandev N, Kagan V, Daoud A, 2010, “Electromagnetic DC pump of liquid aluminium: Computer Simulation and Experimental Study,” Tech Science Press, 3, vol.6, pp. 291-318.

[19] Borges E M, Braz Filho F A, Guimaraes L N F, 2010, “Liquid metal flow control by DC electromagnetic pumps,” Thermal Engineering, vol. 9, pp. 47-54.

[20] Ma K Q, Liu J, 2007, “Heat driven liquid metal cooling device for the thermal management of computer chip,” J Phys D: Apply Phys, 40, pp. 4722-4729.

[21] Zrodnikov A V, Efanov A D, Orlov Y I, 2004, “Heavy liquid metal coolant: Lead-bismuth and lead-technology.” Atomic Energy, 97, pp. 534-537.

[22] Sato K, Furutain A, Saito M, 1991, “Melting attack of solid plates by a high-temperature liquid jet II----Erosion behavior by a molten metal jet.” Nucl Eng Des, 132, pp. 171-186.

[23] Smither R K, Forster G A, Kot C A, 1988, “Liquid gallium metal cooling for optical elements with high heat loads,” Nucl Instrum Meth A, 266, pp. 517-524.

[24] Farabolini W, Ciampichette A, Dabbene F, 2006, “Tritium control modeling for a helium cooled lithium-lead blanket of a fusion power reactor.” Fusion Eng Des, 81, pp. 753-762.

[25] Cao A, Yueh P, Lin L, 2005, “Bi-directional micro relays with liquid metal wetted contacts.” In: Proceedings of 18th IEEE International Conference on Micro Electro Mechanical Systems, Miami Beach, FL, USA: IEEE, 371-374.

[26] Sawada T, Naetchaev A, Ninokata H, 2000, “Gallium-cooled liquid metallic-fueld fast reactor,” Prog Nucl Energ, 37, pp. 313-319.

[27] Nisoli M, Stagira S, Silverstri S D, 1997, “Ultrafast electronic dynamics in solid and liquid gallium nanoparticles”, Phys Rev Lett, 78, pp. 3575-3578.

[28] Liu J, Zhou Y X, Lv Y G, Li T, 2005, “Liquid metal based miniaturized chip cooling device driven by electromagnetic pump,” ASME International Mechanical Engineering Congress and Exposition, .

[29] Liu J, Zhou Y X, Lv Y G, Li T, 2006, “A power way of cooling computer chip using liquid metal with low melting point as the cooling fluid,” Forsch Ingenieuswes, 70, pp. 243-251.

[30] Liu J, Ma K Q, 2007, “Heat driven liquid metal cooling device for the thermal management of a computer chip,” Applied Physics, 40, pp. 4722-4729.

[31] Liu J, Zhou Y X, Ma K Q, 2008, “Power Characteristics of heat driven liquid metal chip cooling device,” Journal of Engineering Thermophysics, 09, pp. 1588-03.

[32] Liu J, Deng Y G, 2010, “Design of Practical liquid metal cooling device for heat dissipation of high performance CPUs,” ASME, vol. 132, 031009-1.

[33] Park C, Jaura AK, 2003, “Dynamic thermal model of li-ion battery for predictive behavior in hybrid and fuel cell vehicle,” SAE technical paper.

[34] Pesaran AA, Vlahinos A, Burch SD, 1997, “Thermal performance of EV and HEV battery modules and packs.”

[35] Liu J, Deng Y G, 2010, “A liquid metal cooling system for the thermal management of high power LEDs,” International Communication in Heat and Mass Transfer, 37, pp. 788-791.

[36] Liu J, Tan S C, Yang X H, 2016, “Thermal management of Li-ion battery with liquid metal,” Energy Conversion and Management, 117, pp. 577-585.

[37] Incropera F P, Dewitt D P, 1996, Fundamentals of Heat and Mass Transfer, 5th edition, John Wiley & Sons.

[38] David H T, Ray W F, 1959, “Performance characteristics of an electromagnetic pump,” Chemistry-General UC-4.